



ACADEMIC  
PRESS

Available online at [www.sciencedirect.com](http://www.sciencedirect.com)

SCIENCE @ DIRECT®

NeuroImage

NeuroImage 20 (2003) 233–243

[www.elsevier.com/locate/ynimg](http://www.elsevier.com/locate/ynimg)

## A mathematical approach to the temporal stationarity of background noise in MEG/EEG measurements

Fetsje Bijma,<sup>a,\*</sup> Jan C. de Munck,<sup>a</sup> Hilde M. Huizenga,<sup>b</sup> and Rob M. Heethaar<sup>c</sup>

<sup>a</sup> MEG Center, Department PMT, VU University Medical Center, De Boelelaan 1118, 1081 HZ Amsterdam, The Netherlands

<sup>b</sup> Department of Developmental Psychology, University of Amsterdam, Roeterstraat 15, 1018 WB Amsterdam, The Netherlands

<sup>c</sup> Department PMT, VU University Medical Center, De Boelelaan 1118, 1081 HZ Amsterdam, The Netherlands

Received 17 September 2002; revised 24 January 2003; accepted 8 April 2003

### Abstract

The general spatiotemporal covariance matrix of the background noise in MEG/EEG signals is huge. To reduce the dimensionality of this matrix it is modeled as a Kronecker product of a spatial and a temporal covariance matrix. When the number of time samples is larger than, say,  $J = 500$ , the iterative Maximum Likelihood estimation of these two matrices is still too time-consuming to be useful on a routine basis. In this study we looked for methods to circumvent this computationally expensive procedure by using a parametric model with subject-dependent parameters. Such a model would additionally help with interpreting MEG/EEG signals. For the spatial covariance, models have been derived already and it has been shown that measured MEG/EEG signals can be understood spatially as random processes, generated by random dipoles. The temporal covariance, however, has not been modeled yet, therefore we studied the temporal covariance matrix in several subjects. For all subjects the temporal covariance shows an alpha oscillation and vanishes for large time lag. This gives rise to a temporal noise model consisting of two components: alpha activity and additional random noise. The alpha activity is modeled as randomly occurring waves with random phase and the covariance of the additional noise decreases exponentially with lag. This model requires only six parameters instead of  $\frac{1}{2}J(J + 1)$ . Theoretically, this model is stationary but in practice the stationarity of the matrix is highly influenced by the baseline correction. It appears that very good agreement between the data and the parametric model can be obtained when the baseline correction window is taken into account properly. This finding implies that the background noise is in principle a stationary process and that nonstationarities are mainly caused by the nature of the preprocessing method. When analyzing events at a fixed sample after the stimulus (e.g., the SEF N20 response) one can take advantage of this nonstationarity by optimizing the baseline window to obtain a low noise variance at this particular sample.

© 2003 Elsevier Science (USA). All rights reserved.

**Keywords:** Magnetoencephalography; Spatiotemporal covariance; Temporal stationarity; Alpha activity

### Introduction

Background noise in MEG/EEG measurements is correlated both in space and in time. When estimating dipole source parameters one has to take into account this noise covariance. The study of the background noise is also important for its own sake because there is still a debate regarding the meaning of averaged brain responses in relation to the background noise (Makeig et al., 2002; Truccolo

et al., 2002; Jaśkowski and Verleger, 2002; Pham et al., 1987). When it is assumed that the recorded signal is a simple superposition of the brain response and the background noise, the Signal Plus Noise (SPN) model, the measured signal  $R_{ij}^k$  at channel  $i$  and time sample  $j$  in trial  $k$  is modeled as

$$R_{ij}^k = R_{ij} + \varepsilon_{ij}^k, \quad (1)$$

where  $R_{ij}$  is the brain response caused by the stimulus and  $\varepsilon_{ij}^k$  the measured noise. The SPN model is based on the assumption that the brain response  $R_{ij}$  does not vary over trials. In general the background noise,  $\varepsilon_{ij}^k$ , can be correlated both in space and in time.

\* Corresponding author. Fax: +31-20-4444147.

E-mail address: [f.bijma@vumc.nl](mailto:f.bijma@vumc.nl) (F. Bijma).

The spatial part has already been studied in detail (Lütkenhöner, 1998a, 1998b; Sekihara et al., 1994; Waldorp et al., 2002; Huizenga and Molenaar, 1995); it has been shown that the accuracy of the estimated source parameters is improved by taking into account this spatial covariance in the localization method. Recently the temporal noise covariance has been incorporated in addition to the spatial covariance. It was demonstrated in Huizenga et al. (2002) and De Munck et al. (2002) that this generally improves the dipole estimation further. Both approaches are based on the SPN model. Moreover, the spatiotemporal noise covariance matrix  $\Sigma$  is modeled as the Kronecker product of a spatial covariance matrix  $X$  and a temporal covariance matrix  $T$  to reduce the dimensionality of the parameter space to a feasible size (De Munck et al., 1992):

$$\Sigma = X \otimes T. \quad (2)$$

Note that  $X$  and  $T$  are not unique due to a common factor; therefore one is normalized. Furthermore, different trials  $k$  and  $k'$  are assumed to be uncorrelated. The Kronecker product assumes that the noise covariance between two measurements at channels  $i$  and  $i'$  at time samples  $j$  and  $j'$ , respectively, is the product of a spatial factor  $X_{ii'}$  and a temporal factor  $T_{jj'}$ :

$$E(\varepsilon_{ij}^k \varepsilon_{i'j'}^{k'}) = \sum_{ij, i'j'} \delta_{k,k'} = X_{ii'} T_{jj'} \delta_{k,k'}, \quad (3)$$

denoting the Kronecker delta function by  $\delta_{k,k'}$ .

In Huizenga et al. (2002) a parametric model is used for both  $X$  and  $T$ , where the matrix elements are assumed to depend only on sensor distance and time difference, respectively. In De Munck et al. (2002) Maximum Likelihood (ML) estimates are derived for  $R$ ,  $X$ , and  $T$  without further assumptions. This yields the estimator for the brain response

$$\hat{R} = \frac{1}{K} \sum_{k=1}^K R^k \quad (4)$$

(the usual averaged signal) and the iterative estimation procedure for the covariance matrices:

$$\hat{X} = \frac{1}{JK} \left[ \sum_{k=1}^K R^k \hat{T}^{-1} (R^k)^t - \hat{R} \hat{T}^{-1} \hat{R}^t \right] \text{ and} \quad (5)$$

$$\hat{T} = \frac{1}{IK} \left[ \sum_{k=1}^K (R^k)^t \hat{X}^{-1} R^k - \hat{R}^t \hat{X}^{-1} \hat{R} \right], \quad (6)$$

where  $I$ ,  $J$ , and  $K$  are the number of channels, time samples, and trials, respectively, and  $R^k$  is the  $(I \times J)$  data matrix of the  $k^{\text{th}}$  trial.  $A^t$  denotes the transpose and  $A^{-1}$  the inverse of matrix  $A$ .

The statistics of  $\varepsilon_{ij}^k$  express properties of the ongoing background activity. If the background noise is modeled as the magnetic/electric field of randomly distributed stationary dipole sources, with the assumptions made that these dipoles are statistically independent and that the source

positions are independent of the source time functions, then the spatiotemporal covariance presents itself as a Kronecker product of a spatial and temporal covariance [Eq. (2)] (De Munck et al., 1992).

For the spatial part of this Kronecker product, models have been described previously (De Munck et al., 1992; De Munck and Van Dijk, 1999). In De Munck et al. (1992) further assumptions were made to describe the spatial part while the temporal part was explicitly left unspecified. The model for the spatial covariance derived in that study can be interpreted mainly as a function of sensor distance (Huizenga et al., 2002; De Munck et al., 2002). It is a natural question whether the temporal covariance has a similar stationarity property. This would mean that the temporal covariance only depends on time difference and is independent of time, so that  $T$  is Toeplitz, i.e., constant along subdiagonals (Huizenga et al., 2002).

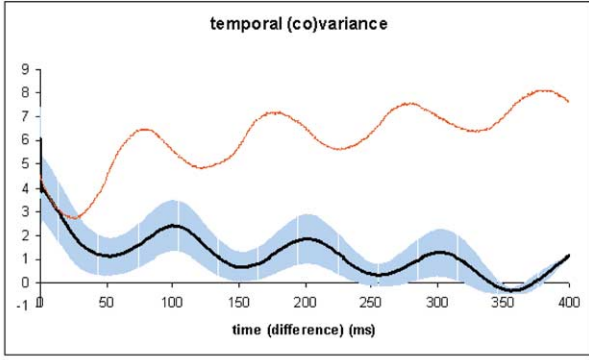
The ML estimation of  $\hat{X}$  and  $\hat{T}$  [Eqs. (5) and (6)] is very time consuming (typically 4 h per iteration on a P3 800 MHz for 1000 time samples, 150 channels, and 500 trials, approximately 18 iterations per estimation). Therefore, parametrization of the noise covariance beyond the Kronecker product with subject-dependent parameters would be favorable also for this reason.

To investigate the possibility of a physiologically adequate parametric model for  $T$ , Eqs. (4) to (6) were applied to several data sets; Fig. 1 shows one example of  $\hat{T}$ . The matrix can be visualized by plotting the average along subdiagonals as function of time difference. For the  $j_0^{\text{th}}$  subdiagonal this average is

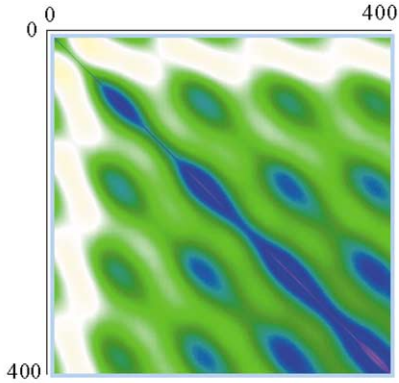
$$\frac{1}{J - j_0} \sum_{j=0}^{J-j_0-1} T_{j, j+j_0} \quad (7)$$

In Fig. 1a this average covariance (black line) and its standard deviation (blue band) are plotted as a function of time lag together with the diagonal of  $\hat{T}$  (red line), i.e., the variance, as function of time. In Fig. 1b the same matrix is plotted as bitmap. From this illustration it is clear that it is not correct to assume the temporal covariance to be stationary.

First of all, the variance in Fig. 1a is not constant over time but oscillates. The oscillation in the average covariance (black line in Fig. 1a) does not indicate nonstationarity but can be explained by alpha activity: time differences of a multiple of alpha periods show higher covariance values. However, the SD band around the average covariance witnesses nonstationarity: the rather high and fluctuating SD shows that on some subdiagonals the variation around the average covariance is higher than on others. In Fig. 1b the oscillations in both the diagonal and the antidiagonal direction (the oscillating subdiagonals and the oscillating average covariance) result in blue spots in the figure, while in the case of temporal stationarity one would expect a line pattern (one color per subdiagonal). In all, Fig. 1 shows an example of a nonstationary matrix.



(a)



(b)

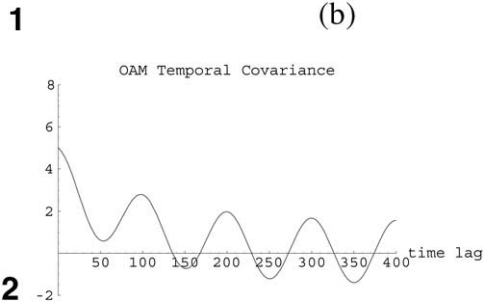


Fig. 1. Two different visualizations of the same ML-estimated temporal covariance matrix. (a) Black line, average temporal covariance ( $fT^2$ ) as in Eq. (7) ( $\pm$  SD in the blue band) as a function of time difference (ms). Red line, temporal variance ( $fT^2$ ) as a function of time (ms). The vertical scale is in arbitrary units because of the common factor of  $X$  and  $T$  [Eq. (2)]. (b) The entire temporal covariance matrix (400 ms by 400 ms) plotted as bitmap. Purple indicates highest values, white lowest values.

Fig. 2. The covariance in  $(fT)^2$  of the OAM as a function of time lag (ms) for  $\omega = 20\pi \text{ rad s}^{-1}$ ,  $\Omega^2 = 3 (fT)^2$ ,  $\sigma^2 = 3.5 (fT)^2$ , and  $\kappa = 10\text{s}^{-1}$ .

The oscillations in Fig. 1 suggest that the background noise is (partly) generated by alpha activity. Therefore in the following we propose a parametrization of  $T$  which is based on a noise model consisting of two components: alpha activity and additional random noise. The covariance of this

additional noise is modeled as an exponentially decreasing function of time lag (i.e., as low-frequency noise). The Ongoing Alpha Model (OAM) is based on the assumption of ongoing alpha activity, i.e., one everlasting wave. The Poisson Modulated Alpha Model (PoMAM) assumes that the alpha activity consists of separated waves which occur randomly and have fixed duration. This assumption is more realistic because raw data clearly show separated waves.

Furthermore, the observed nonstationarity is brought into the model by considering the detailed preprocessing of the raw data.

## Methods

### Ongoing alpha model

In the OAM the temporal component of the background noise is modeled as the sum of an ongoing alpha wave and additional random noise. For convenience the model uses continuous time, and is converted to discrete time in its application to our experiment. The formula for the noise in the  $k^{\text{th}}$  trial,  $\varepsilon_k(t)$ , is then given by

$$\varepsilon_k(t) = \Omega \sin(\omega t + \tau_k) + \eta_k(t), \quad (8)$$

where  $\Omega$  (fT) is the amplitude,  $\omega$  ( $\text{rad s}^{-1}$ ) is the frequency of the alpha activity, and  $t$  (s) is time. Because we used a random interstimulus interval the phase of the wave,  $\tau_k$  (rad), is random for each trial; i.e., the stochastic  $\tau_k$  has the uniform distribution in  $[-\pi, \pi]$ . For the additional noise,  $\eta_k(t)$  (fT), we assume

$$E(\eta_k(t_1)\eta_k(t_2)) = \sigma^2 e^{-\kappa|t_2-t_1|} \quad (9)$$

where  $\kappa$  is in  $\text{s}^{-1}$ ,  $\kappa > 0$ , and  $\sigma^2$  is the variance in  $(fT)^2$ . This means that the additional noise is temporally stationary. Furthermore, the alpha wave is assumed to be independent of the additional noise. Now the temporal covariance for an arbitrary trial  $k$  is

$$\begin{aligned} \text{Cov}(t_1, t_2) &= E(\varepsilon_k(t_1) \cdot \varepsilon_k(t_2)) \\ &= E[(\Omega \sin(\omega t_1 + \tau_k) + \eta_k(t_1)) \\ &\quad \times (\Omega \sin(\omega t_2 + \tau_k) + \eta_k(t_2))] \\ &= \frac{\Omega^2}{2\pi} \int_{-\pi}^{\pi} [\sin(\omega t_1 + \tau_k) \\ &\quad \times \sin(\omega t_2 + \tau_k)] d\tau_k + \sigma^2 e^{-\kappa|t_2-t_1|} \\ &= \frac{\Omega^2}{2} \cos(\omega(t_2 - t_1)) + \sigma^2 e^{-\kappa|t_2-t_1|}. \end{aligned} \quad (10)$$

From Eq. (10) it is clear that the OAM is stationary:  $\text{Cov}(t_1, t_2)$  only depends on time lag  $t_2 - t_1$ . Fig. 2 shows

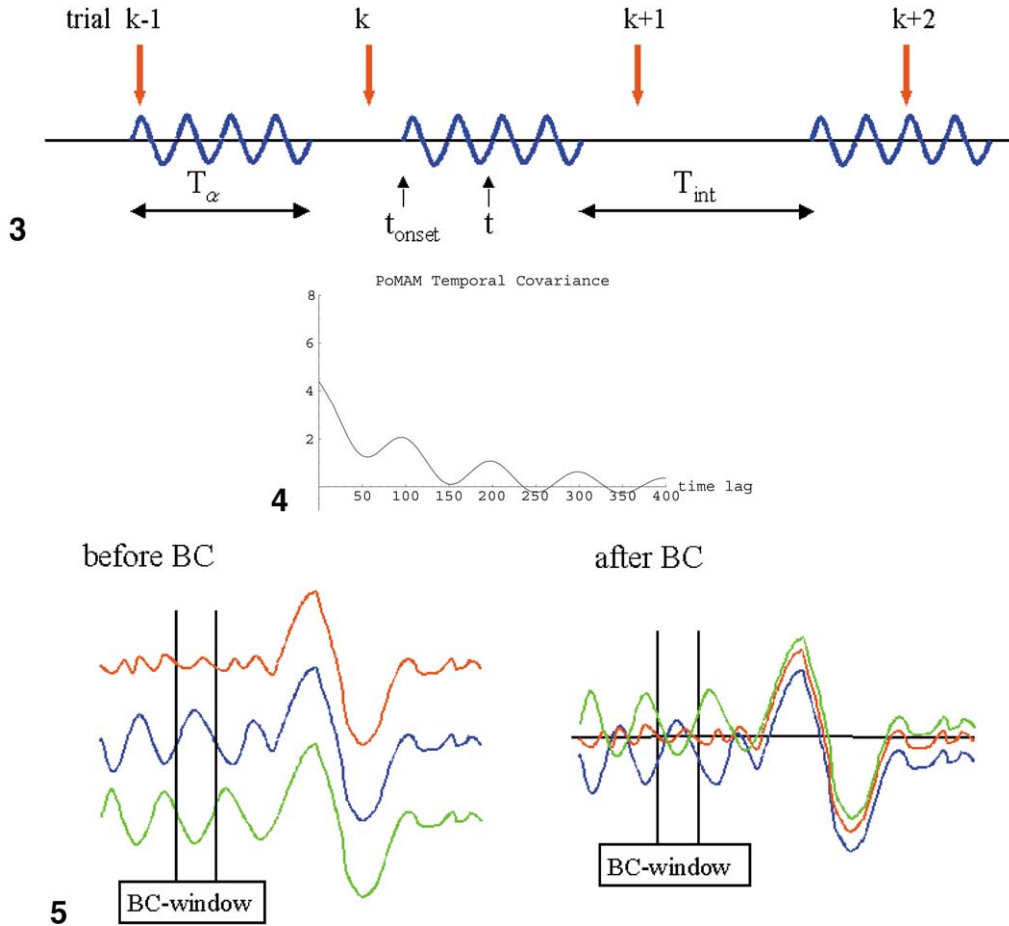


Fig. 3. Alpha waves occurring according to the PoMAM. Because of the random interstimulus interval trial onsets can occur in any phase of the wave.  $T_{\text{int}}$  denotes the time between waves,  $T_{\alpha}$  the duration of a wave.  $t_{\text{onset}}$  indicates the onset of a wave in trial  $k$ .

Fig. 4. The covariance in  $(fT)^2$  of the PoMAM with fixed amplitude as a function of time lag (ms) for  $T_{\alpha} = 600$  ms,  $\lambda = 1/0.6$  s $^{-1}$ ,  $\omega = 20\pi$  rad s $^{-1}$ ,  $\Omega^2 = 3$  ( $fT$ ) $^2$ ,  $\sigma^2 = 3.5$  ( $fT$ ) $^2$ , and  $\kappa = 10$  s $^{-1}$ .

Fig. 5. The effect of the baseline correction on three signals (red, without alpha activity in the BC window; blue and green, with alpha activity in the BC window). When the average alpha activity during the BC window is not zero the BC introduces a vertical shift in the signal (blue and green).

that this covariance does not vanish for large time difference (as in Fig. 1a), but remains oscillatory. For this reason the more realistic Poisson Modulated Alpha Model is introduced.

### Poisson modulated alpha model

In the PoMAM the alpha activity is modulated by an interrupted Poisson process. A Poisson process with intensity parameter  $\lambda$  (s $^{-1}$ ) is a statistical process generating events at random with mean intermediate time  $1/\lambda$  (Chung, 1993; Stirzaker, 1994). The time between two consecutive events has the Exponential( $\lambda$ ) probability density function:

$$f_{\lambda}(t) = \lambda e^{-\lambda t} 1_{[0, \infty)}(t), \quad (11)$$

where  $1_{[a,b]}(t) = 1$  for  $t \in [a, b]$  and zero for  $t \in [a, b]$ .

In the covariance model the events stand for the onsets of alpha waves (Fig. 3) which have fixed duration  $T_{\alpha}$  (s). After

each event the process is disrupted for  $T_{\alpha}$ , the following wave, after which it resumes to generate the next event (onset). Different waves are assumed to be uncorrelated.

In the PoMAM two stochastic processes are operating simultaneously, namely the Poisson process (generating wave onsets) and the random phase process. These two processes are assumed to be statistically independent.

Assuming the amplitude of a wave to be constant and equal to  $\Omega$ , the amplitude time function (envelope) of a wave which started at  $t = 0$  is  $\Omega 1_{[0, T_{\alpha}]}(t)$ . Let  $\varepsilon_k^{\alpha}(t) = \varepsilon_k(t) - \eta_k(t)$  denote the alpha part of the noise. In Fig. 3 the alpha activity at time  $t$  in trial  $k$  due to the wave started at  $t_{\text{onset}}$  is

$$\begin{aligned} \varepsilon_k^{\alpha}(t) &= \Omega 1_{[0, T_{\alpha}]}(t - t_{\text{onset}}) \sin(\omega(t - t_{\text{onset}}) + \tau_k) \\ &= \Omega 1_{[0, T_{\alpha}]}(t - t_{\text{onset}}) \sin(\omega t + \tau'_k), \end{aligned} \quad (12)$$

where  $\tau'_k = -\omega t_{\text{onset}} + \tau_k$  having the same probability density function as  $\tau_k$ , uniformly in  $[-\pi, \pi]$ . Therefore in the sequel  $\tau'_k$  will be denoted as  $\tau_k$  again. From Eq. (12) it is

clear that the Poisson process only comprises the amplitudes of the waves, so that the expected value of the error is still zero because of the random phase  $\tau_k$ .

The covariance in the PoMAM is

$$\begin{aligned} Cov(t_1, t_2) &= E(\varepsilon_k(t_1) \cdot \varepsilon_k(t_2)) \\ &= Cov^\alpha(t_1, t_2) + Cov^\eta(t_1, t_2) \end{aligned} \quad (13)$$

because the alpha activity and the additional noise are assumed to be independent. The second term is the same as in the OAM

$$Cov^\eta(t_1, t_2) = \sigma^2 e^{-\kappa|t_2 - t_1|}. \quad (14)$$

The computation of the alpha part of the covariance is complicated because there are different possibilities for  $t_1$  and  $t_2$ . First, if  $t_1$  and  $t_2$  are in the same wave, then  $Cov^\alpha(t_1, t_2) \neq 0$  in general. Second, if one of the two instants, say  $t_1$ , is in a wave, and  $t_2$  is not in the same wave (not in any wave or perhaps in another wave), then  $Cov^\alpha(t_1, t_2) = 0$ , because either  $\varepsilon_k^\alpha(t_2) = 0$  or  $t_2$  is in another wave, and different waves are assumed to be independent. And finally, if both instants are not in any wave,  $Cov^\alpha(t_1, t_2) = 0$ , obviously. Therefore only the case of  $t_1$  and  $t_2$  being in the same wave has to be considered.

In order to compute the covariance of the PoMAM the Total Probability Theorem (Chung, 1993) applied to a function  $g$  of a stochastic  $X$  is used:

$$\begin{aligned} E(g(X)) &= P(A) \cdot E(g(X)|A) \\ &\quad + P(A^c) \cdot E(g(X)|A^c), \end{aligned} \quad (15)$$

where  $A^c$  stands for the complement of event  $A$ . Defining  $A$  to be the event “ $t_1$  and  $t_2$  are in the same wave” and  $g(X)$  to be  $\varepsilon_k^\alpha(t_1)\varepsilon_k^\alpha(t_2)$ , which is a function of both stochastic processes, Eq. (15) yields

$$\begin{aligned} Cov^\alpha(t_1, t_2) &= E(\varepsilon_k^\alpha(t_1) \cdot \varepsilon_k^\alpha(t_2)) \\ &= P(A) \cdot E(\varepsilon_k^\alpha(t_1) \varepsilon_k^\alpha(t_2)|A). \end{aligned} \quad (16)$$

In this formula the results from Appendix 1 ( $P(A)$ ) and Appendix 2 ( $E(\varepsilon_k^\alpha(t_1)\varepsilon_k^\alpha(t_2)|A)$ ) are substituted [Eqs. ((A.4) and (B.2))]:

$$\begin{aligned} Cov^\alpha(t_1, t_2) &= \lambda(T_\alpha - |t_2 - t_1|) e^{\lambda T_\alpha} \Gamma(0, \lambda T_\alpha) \frac{\Omega^2}{2} \\ &\quad \times \cos(\omega(t_2 - t_1)) 1_{[-T_\alpha, T_\alpha]}(t_2 - t_1). \end{aligned} \quad (17)$$

This can be written as

$$\begin{aligned} Cov^\alpha(t_1, t_2) &= \lambda T_\alpha e^{\lambda T_\alpha} \Gamma(0, \lambda T_\alpha) \frac{T_\alpha - |t_2 - t_1|}{T_\alpha} \\ &\quad \times 1_{[-T_\alpha, T_\alpha]}(t_2 - t_1) \frac{\Omega^2}{2} \cos(\omega(t_2 - t_1)) \end{aligned}$$

$$\begin{aligned} &= \gamma(\lambda, T_\alpha) \frac{\Omega^2(T_\alpha - |t_2 - t_1|)}{T_\alpha} 1_{[-T_\alpha, T_\alpha]}(t_2 - t_1) \\ &\quad \times \frac{1}{2} \cos(\omega(t_2 - t_1)), \end{aligned} \quad (18)$$

where

$$\gamma(\lambda, T_\alpha) = \lambda T_\alpha e^{\lambda T_\alpha} \Gamma(0, \lambda T_\alpha). \quad (19)$$

One can regard Eq. (18) as the product of three factors:  $\gamma(\lambda, T_\alpha)$ , which is the probability that at least one instant is in a wave (cf. Appendix 1 with  $t_1 = t_2$ ), the convolution of the amplitudes, and the covariance of the OAM with unit amplitude.

In all, we have the total PoMAM covariance

$$\begin{aligned} Cov(t_1, t_2) &= \gamma(\lambda, T_\alpha) \frac{\Omega^2(T_\alpha - |t_2 - t_1|)}{T_\alpha} \\ &\quad \times 1_{[-T_\alpha, T_\alpha]}(t_2 - t_1) \frac{1}{2} \cos(\omega(t_2 - t_1)) \\ &\quad + \sigma^2 e^{-\kappa|t_2 - t_1|}. \end{aligned} \quad (20)$$

Note that this expression is entirely parametric.

From Eq. (20) it is clear that the PoMAM is a stationary model; the formula only depends on lag  $t_2 - t_1$ .

For a more general envelope function of the waves  $\Phi(t)$  the covariance can be calculated in a similar way. The convolution of the amplitudes then becomes

$$\frac{1}{T_\alpha} \int_0^{T_\alpha} \Phi(s) \Phi(s + |t_2 - t_1|) ds \quad (21)$$

and the equivalent of Eq. (20) becomes

$$\begin{aligned} Cov(t_1, t_2) &= \gamma(\lambda, T_\alpha) \frac{1}{T_\alpha} \int_0^{T_\alpha} \Phi(s) \Phi(s + |t_2 - t_1|) ds \\ &\quad \frac{1}{2} \cos(\omega(t_2 - t_1)) + \sigma^2 e^{-\kappa|t_2 - t_1|}. \end{aligned} \quad (22)$$

An example of the PoMAM with fixed amplitude is plotted in Fig. 4. We see that for the PoMAM the covariance indeed vanishes for big time lags as in Fig. 1a.

### Baseline correction

Due to external influences in MEG/EEG measurements the baselines of the single-channel signals are usually shifted over an unknown offset which can be quite large. To correct for these shifts one has to carry out an offset removal. One standard way of performing this baseline correction (BC) is to subtract per channel the average over a prestimulus interval. In this section the influence of this preprocessing on the temporal covariance matrix is studied.

Let  $[t_0 - T_c, t_0]$  be the interval over which the correction is calculated. The formula for the corrected noise of the  $k^{\text{th}}$  trial,  $\varepsilon_k^c(t)$ , is then

$$\varepsilon_k^c(t) = \varepsilon_k(t) - \frac{1}{T_c} \int_{t_0 - T_c}^{t_0} \varepsilon_k(t') dt'. \quad (23)$$

To compute the (co)variance of the corrected signal, the corrected (co)variance, one has to calculate

$$\begin{aligned} Cov^c(t_1, t_2) &= E(\varepsilon_k^c(t_1) \cdot \varepsilon_k^c(t_2)) \\ &= Cov(t_1, t_2) - \frac{1}{T_c} \int_{t_0 - T_c}^{t_0} [Cov(t_1, t') \\ &\quad + Cov(t_2, t')] dt' \\ &\quad + \frac{1}{T_c^2} \int_{t_0 - T_c}^{t_0} \int_{t_0 - T_c}^{t_0} Cov(t', t'') dt' dt''. \end{aligned} \quad (24)$$

The first term in Eq. (24) is the stationary uncorrected covariance and the last term is a constant dependent on  $T_c$  and  $t_0$ . The second term, though, is in general not stationary. In Fig. 5 the effect of the BC is illustrated. If a signal contains alpha activity having nonzero average over the BC window, a vertical shift is introduced by the correction. Moreover, this introduced variance varies with time: the variation in signals is periodically bigger or smaller. If the BC window equals one alpha period, the average alpha activity will be zero and this oscillating additional variance will not occur.

For the OAM formula Eq. (24) can be computed (partly) analytically using Eq. (10) (see Appendix 3):

$$\begin{aligned} Cov^c(t_1, t_2) &= \Omega^2 \left[ \frac{1}{\omega^2 T_c^2} (1 - \cos(\omega T_c)) \right. \\ &\quad + \frac{1}{2} \cos(\omega(t_2 - t_1)) \\ &\quad - \frac{2}{\omega T_c} \sin \frac{\omega T_c}{2} \cos \left( \frac{\omega(t_2 - t_1)}{2} \right) \\ &\quad \left. \times \cos \left( \omega \left( \frac{t_1 + t_2}{2} - t_0 + \frac{T_c}{2} \right) \right) \right] \\ &\quad + \sigma^2 e^{-\kappa|t_2 - t_1|} - \frac{\sigma^2}{T_c} \int_{t_0 - T_c}^{t_0} \\ &\quad (e^{-\kappa|t_1 - t'|} + e^{-\kappa|t_2 - t'|}) dt' \\ &\quad + \frac{\sigma^2}{T_c^2} \int_{t_0 - T_c}^{t_0} \int_{t_0 - T_c}^{t_0} e^{-\kappa|t' - t''|} dt' dt''. \end{aligned} \quad (25)$$

As an example the corrected variance ( $t_1 = t_2 = t$ ) is plotted in Fig. 6 for three different values of  $T_c$  for both the OAM (Fig. 6a) and for empirical data (Fig. 6b). It is clear from these figures that the corrected temporal covariance structure is not stationary and that this nonstationarity highly depends on the choice of baseline correction. Although there are differences between the OAM figure and the empirical figure, the similarity in effect of baseline correction is striking.

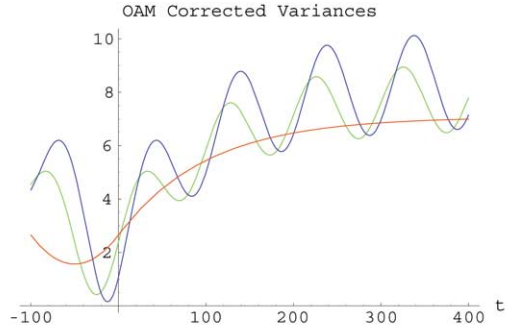
There is an alpha oscillation in the variance for  $T_c = 25$  ms (blue) and  $T_c = 50$  ms (green), but this oscillation vanishes for  $T_c = 100$  ms (red). This is clarified by the term within square brackets of Eq. (25): the amplitude of this sinusoid in  $(t_1 + t_2)/2$  contains the factor  $\sin(\omega T_c/2)$  which is in the case of Fig. 6a equal to  $\sin(T_c \pi/100)$  (taking time in ms) and is zero for  $T_c = 100$  ms. Furthermore the phase of this oscillation is  $-t_0 + T_c/2$ , so the phase shift between the green and the blue line is 12.5 ms. The average variance is minimum for the red line in this figure ( $T_c = 100$  ms) since then  $1/(\omega^2 T_c^2)(1 - \cos(\omega T_c)) = 1/(4\pi^2)[1 - \cos(\pi 100/50)] = 0$ ; see Eq. (25).

The variance is minimum at  $t = -T_c/2$ , the centre of the preprocessing window, in all cases. This drop is caused by the second half of Eq. (25), taking  $t_1 = t_2 = t$ . This corrected variance due to  $\eta(t)$  consists of a constant, a nonstationary term, and another constant. The integrand in the middle term is larger for  $t$  closer to the correction window, because then  $|t - t'|$  is smaller. Therefore the closer  $t$  is to this window, the larger the integral. Together with the minus sign in front of the term, this causes the drop. Moreover, a decrease in  $T_c$  increases the magnitude of the drop (see Appendix 4).

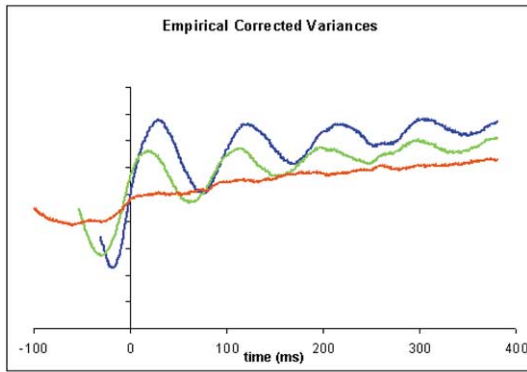
To obtain stationarity one should choose  $T_c$  in such a way that the oscillation vanishes and the drop is minimum. This is achieved when  $\omega T_c = 2l\pi$ ,  $l \in \mathbb{N}$ ; i.e., when the correction interval is taken to be  $l$  alpha periods with  $l \in \mathbb{N}$ . The bigger  $l$ , the smaller the magnitude of the drop, thus the more stationary the matrix. To keep the preprocessing feasible taking one or two alpha periods as the preprocessing window is adequate.

If one is interested in a particular sample after the stimulus (e.g., the N20 response in a somatosensory evoked field (SEF) experiment), advantage can be taken of the nonstationarity due to the BC. In Fig. 7 the empirical variances at  $t = 20$  ms and  $t = 60$  ms after the stimulus in a SEF data set are plotted for several values of  $T_c$ . It becomes clear in this figure that for the N20 response the optimal BC length is 100 ms, while for  $t = 60$  ms a BC window of 70 ms yields the minimum variance. This can be explained by Eq. (25): if the time sample  $t$  and the PoMAM parameters are substituted then this formula becomes a parametric expression in  $t_0$  and  $T_c$ , which can be minimized with respect to  $T_c$ , taking  $t_0 = 0$ .

The covariance of the corrected error  $\varepsilon_k^c(t)$  in the PoMAM is calculated using Eqs. (20) and (24). For the PoMAM with fixed amplitude Eq. (24) becomes a parametric



(a)



(b)

Fig. 6. Corrected OAM variance and corrected empirical variance for three different values of  $T_c$ . (a) The corrected OAM variance as a function of  $t$  in ms with  $\omega = 20\pi \text{ rad s}^{-1}$ ,  $\tilde{\Omega}^2 = 2(fT)^2$ ,  $\sigma^2 = 3.5(fT)^2$ ,  $\kappa = 10 \text{ s}^{-1}$ , and  $t_0 = 0 \text{ ms}$  for different values of  $T_c$ . The blue line corresponds to  $T_c = 25 \text{ ms}$ , the green line to  $T_c = 50 \text{ ms}$ , and the red line to  $T_c = 100 \text{ ms}$ . (b) Corrected empirical variances. The colors and values for  $T_c$  and  $t_0$  are the same as in (a).

representation for the entries of the temporal covariance matrix  $T$ . The main difference between the simple OAM model and this parametric PoMAM is the decrease in amplitude of the oscillations in the (co)variance. The effect of the baseline correction on the stationarity is the same for both models. Therefore it is sufficient to examine Eq. (25) for the simpler OAM instead of the more complicated Eq. (24) to investigate stationarity of the PoMAM.

## Results

The PoMAM was fitted to ML-estimated temporal covariance matrices of five subjects to see how well this parametric model describes the abstract and nonphysiological ML estimate. The ML estimates were obtained from MEG data of SEF experiments where the left median nerve

was stimulated. Data were acquired on a 151-channel CTF Omega system at a sample rate of 2 kHz. No filtering was applied, except for the baseline correction. Subjects 2 and 3 were stimulated at a constant stimulus rate of 1 Hz, while the interstimulus interval in Subjects 1, 4, and 5 varied uniformly between 800 and 1200 ms. In our experiments we found that the best fitting values for the model parameters reproduce very well between data sets with random and regular stimulation within subjects. Therefore the comparison of parameter values for Subjects 2 and 3 with those for the other subjects is justified. The number of trials was approximately 500 for all subjects.

The parameters  $\lambda$  (the intensity of the Poisson process) and  $\Omega$  (the amplitude of the waves) were fitted simultaneously in  $\tilde{\Omega}^2 \equiv \lambda T_\alpha e^{\lambda T_\alpha} \Gamma(0, \lambda T_\alpha) \Omega^2$ , for they cannot be distinguished in the covariance Eq. (18). Furthermore, an additional term  $\sigma_{hf}^2$  was added to the main diagonal and  $\frac{1}{2}\sigma_{hf}^2$  to the first subdiagonal to model high-frequency noise due to the omitted filtering. The parameters to be fitted for are  $\omega$  (alpha frequency),  $T_\alpha$  (duration of alpha wave),  $\kappa$  (covariance length of additional noise),  $\sigma^2$  [variance of additional (low-frequency) noise],  $\sigma_{hf}^2$  (variance due to high-frequency noise), and  $\tilde{\Omega}^2$  (representing amplitude and intensity of alpha activity).

The cost function used is

$$C(\omega, T_\alpha, \kappa, \tilde{\Omega}^2, \sigma^2, \sigma_{hf}^2) = \frac{\sum_{t_1} \sum_{t_2} [T_{(\omega, T_\alpha, \kappa, \tilde{\Omega}^2, \sigma^2, \sigma_{hf}^2)}(t_1, t_2 | t_0, T_c) - \hat{T}(t_1, t_2)]^2}{\sum_{t_1} \sum_{t_2} [\hat{T}(t_1, t_2)]^2} \times 100\%, \quad (26)$$

i.e., the relative squared Frobenius norm of the difference between the model matrix  $T$  and the ML-estimated matrix  $\hat{T}$ . We used the Simplex method to minimize [Eq. (26)]. Only the three nonlinear parameters ( $\omega$ ,  $T_\alpha$ ,  $\kappa$ ) were estimated by this iterative method; the three linear parameters ( $\tilde{\Omega}^2$ ,  $\sigma^2$ ,  $\sigma_{hf}^2$ ) were fitted in a least-squares sense in each iteration. The values for  $t_0$  and  $T_c$  were taken to be equal to the values taken in the ML procedure. In our experiment we did not strive for stationary matrices; instead we attempted to approximate as accurately as possible the ML-estimated matrices irrespective of the correction window used. Moreover,

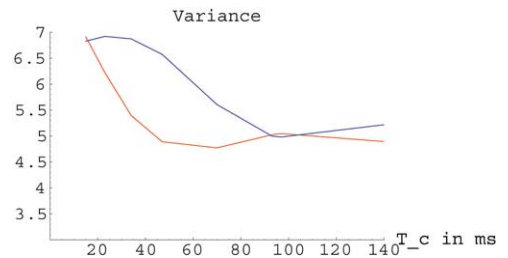


Fig. 7. The empirical variance of a SEF data set at  $t = 20 \text{ ms}$  (blue line) and  $t = 60 \text{ ms}$  (red line) after the stimulus for different values of  $T_c$  (length of the BC window);  $t_0 = 0$ .

Table 1  
Best-fitting-values for the six parameters of the Poisson Modulated Alpha Model together with the residual error for five different subjects

Subject	Stim	$T_c$	$\frac{\omega}{2\pi}$	$T_\alpha$	$\frac{1}{\kappa}$	$\Omega^2$	$\sigma^2$	$\sigma_{hf}^2$	$C$
1	Random	48	10.61	287	22.9	19980	13610	21099	0.4%
2	Regular	25	9.85	359	73.8	23527	15382	22952	0.5%
3	Regular	50	11.03	289	16.3	22651	12274	16804	0.7%
4	Random	50	8.85	536	14.7	8497	10402	11787	0.6%
5	Random	49	11.92	61	85.3	24746	11746	17293	0.4%
Average			10.45	306	42.6	19880	12683	17987	0.58%
Unit		ms	Hz	ms	ms	(fT) <sup>2</sup>	(fT) <sup>2</sup>	(fT) <sup>2</sup>	

*Note.* The number of time samples is 500. The values for  $t_0$  and  $T_c$  were taken equal to their corresponding values in the ML-estimated matrices. Subjects 2 and 3 had their eyes open; the others had their eyes closed.

it can be verified in this way whether the effect of the baseline correction is taken into account correctly.

The best-fitting parameter values together with the cost function values for the five subjects are stated in Table 1. This table shows that our model describes the temporal covariance structure accurately: the ML-estimated matrices can be approximated up to an error of less than 1% in relative squared Frobenius norm by the PoMAM.

In our estimation the nonlinear parameters  $T_\alpha$  and  $\kappa$  appeared to be rather insensitive, while the parameter  $\omega$  was most sensitive.

## Discussion

The temporal covariance of the background noise in MEG/EEG measurements can be described accurately by the parametric PoMAM. In the PoMAM the temporal noise is modeled in a physiological way as the sum of randomly occurring alpha waves and additional noise. In principle this model is stationary, but in practice the temporal stationarity is hampered by the baseline correction, which is apparent from Fig. 5 and Eqs. (24) and (25). Taking this preprocessing into account properly, the ML-estimated temporal covariance matrix can be described up to an error of less than 1% (Table 1) using only six parameters.

Some parameters (especially  $T_\alpha$  and  $\kappa$ ) appeared to be rather insensitive. This redundancy shows that a model with even less parameters is possible. Taking these insensitive parameters into account, we expect that it will be possible to compose a *standard* PoMAM matrix  $T$  (based on standard values for  $T_\alpha$ ,  $\kappa$ ,  $\Omega$ ,  $\sigma$ , and  $\sigma_{hf}$ , but still depending on the sensitive parameter  $\omega$ ) which will function considerably better in source localization than  $T = \sigma^2 I$  does.

However, it is not straightforward how to estimate the PoMAM parameters based on raw data. A detailed comparison between the computational expense of the ML estimates and the PoMAM will be made in a future study.

The temporal stationarity of the background noise highly

depends on the window used for the baseline correction [Eq. (25)]. Taking the length of this window to be equal to a multiple of alpha periods, one obtains the most stationary temporal covariance. However, for a fixed sample this does not always yield the minimum variance (Fig. 7). Therefore one can optimize the baseline correction window in order to minimize the variance for a certain sample of interest.

Even in analyses where no temporal correlations are taken into account [i.e., assuming  $Cov(t_1, t_2) = \sigma^2 \delta(t_1 - t_2)$ ], the baseline correction alters the covariance matrix. In that case it is inconsistent to just fix the baseline corrected temporal covariance matrix to  $\sigma^2 I$ , because due to the correction a positive constant is added to all entries in  $T$  [see Eq. (24)].

In Truccolo et al. (2002) it is shown that trial-to-trial variations in the response cause nonstationarities in the background noise when trials are averaged according to the SPN model. In our SEF experiment the assumption of the SPN model leads to temporally stationary background noise; the observed nonstationarity in the matrix is caused by the preprocessing and does not originate from the data (Makeig et al., 2002). Therefore our methods, which contrary to others are based on both spatial and temporal correlations of the background noise, show no reasons to reject the SPN model.

In the PoMAM the alpha activity is modeled as a random phase process with constant amplitude. If alpha waves were modulated by the stimulus one would expect a different probability density function for the phase  $\tau_\kappa$  and possibly a different amplitude time function for the waves [as in Eq. (22)] (Makeig et al., 2002). The small fit error of the PoMAM (Table 1) shows that our data can be well understood without the assumption of such a stimulus-modulated alpha model.

In all we have derived a mathematical model, the Poisson Modulated Alpha Model, describing the temporal noise covariance in a physiological and accurate way. For practical application of this model further study of the parameter estimation and the effect on source localization is needed.

**Acknowledgment**

The authors thank Dr. K. Böcker for carefully reading the manuscript and giving helpful suggestions.

**Appendix 1**

In this appendix the probability that two instants,  $t_1$  and  $t_2$ , are in the same alpha wave is computed. First  $t_1 < t_2$  is assumed. For  $t_2 - t_1 > T_\alpha$  this probability is obviously zero. For  $t_2 - t_1 < T_\alpha$  the probability is derived below.

If the intermediate time between waves were fixed to  $T_{int}$  the probability that both instants are in the same wave would be equal to the ratio

$$\frac{T_\alpha - (t_2 - t_1)}{T_\alpha + T_{int}}. \tag{A.1}$$

One can regard Eq. (A.1) as the ratio between favorable instants for  $t_1$  and all possible instants. By the assumption that the alpha waves are generated by a Poisson process the intermediate time  $T_{int}$  has an Exponential( $\lambda$ ) distribution. The above probability [Eq. (A.1)] can be interpreted as a function of the stochast  $T_{int}$ . The expected value of a function  $g(X)$  of a stochast  $X$  with probability density function  $f_x(x)$  is (Chung, 1993):

$$E(g(X)) = \int_{-\infty}^{\infty} g(x) f_x(x) dx. \tag{A.2}$$

Combining Eqs. (11), (A.1), and (A.2) we obtain

$$\begin{aligned} P(t_1 \text{ and } t_2 \text{ in same wave}) &= E_{T_{int}}(P_{T_{int}}(t_1 \text{ and } t_2 \text{ in same wave})) \\ &= \int_0^\infty \frac{T_\alpha - (t_2 - t_1)}{T_\alpha + \theta} \lambda e^{-\lambda\theta} d\theta \\ &= \lambda(T_\alpha - (t_2 - t_1)) e^{\lambda T_\alpha} \int_{T_\alpha}^\infty \frac{1}{\theta'} e^{-\lambda\theta'} d\theta' \\ &= \lambda(T_\alpha - (t_2 - t_1)) e^{\lambda T_\alpha} \Gamma(0, \lambda T_\alpha), \end{aligned} \tag{A.3}$$

where  $\Gamma$  is the incomplete gamma function  $\Gamma(0, a) = \int_a^\infty (1/\theta) e^{-\theta} d\theta$ . For arbitrary values of  $t_1$  and  $t_2$  this results in

$$\begin{aligned} P(t_1 \text{ and } t_2 \text{ in same wave}) &= \lambda(T_\alpha - |t_2 - t_1|) e^{\lambda T_\alpha} \Gamma(0, \lambda T_\alpha) 1_{[-T_\alpha, T_\alpha]}(t_2 - t_1). \end{aligned} \tag{A.4}$$

**Appendix 2**

In this appendix the last term of Eq. (16):

$$E(\varepsilon_k^\alpha(t_1) \varepsilon_k^\alpha(t_2) | t_1 \text{ and } t_2 \text{ in same wave})$$

is calculated. From Eq. (12) it is clear that the onset of the wave in which  $t_1$  and  $t_2$  occur determines the amplitude of the activity at both instants. Therefore all possible onsets have to be taken into account. First assume  $t_1 < t_2$ . Given the event “ $t_1$  and  $t_2$  are in the same wave” the stochast  $S = t_1 - t_{\text{onset}}$  has a uniform distribution in  $[0, T_\alpha - (t_2 - t_1)]$ . Using Eq. (A.2) with  $S$  as stochast and  $\varepsilon_k^\alpha(t_1) \varepsilon_k^\alpha(t_2)$ , the function, yields

$$\begin{aligned} E(\varepsilon_k^\alpha(t_1) \varepsilon_k^\alpha(t_2) | t_1 \text{ and } t_2 \text{ in same wave, } t_1 < t_2) &= \frac{1}{2\pi} \int_{-\pi}^\pi \left[ \frac{\Omega^2}{T_\alpha - (t_2 - t_1)} \int_0^{T_\alpha - (t_2 - t_1)} 1_{[0, T_\alpha]}(s) \right. \\ &\quad \times \sin(\omega t_1 + \tau_k) 1_{[0, T_\alpha]}(s + t_2 - t_1) \\ &\quad \left. \times \sin(\omega t_2 + \tau_k) ds \right] d\tau_k \\ &= \frac{\Omega^2}{2} \cos(\omega(t_2 - t_1)). \end{aligned} \tag{B.1}$$

Taking  $t_1$  and  $t_2$  as arbitrary in the same wave, this remains

$$\begin{aligned} E(\varepsilon_k^\alpha(t_1) \varepsilon_k^\alpha(t_2) | t_1 \text{ and } t_2 \text{ in same wave}) &= \frac{\Omega^2}{2} \cos(\omega(t_2 - t_1)). \end{aligned} \tag{B.2}$$

**Appendix 3**

For the simplified OAM the corrected covariance [Eq. (24)] is calculated using the covariance for the uncorrected case [Eq. (10)]:

$$\begin{aligned} Cov^c(t_1, t_2) &= Cov(t_1, t_2) - \frac{1}{T_c} \int_{t_0 - T_c}^{t_0} \\ &\quad [Cov(t_1, t') + Cov(t_2, t')] dt' \\ &\quad + \frac{1}{T_c^2} \int_{t_0 - T_c}^{t_0} \int_{t_0 - T_c}^{t_0} Cov(t', t'') dt' dt'' \\ &= \frac{\Omega^2}{2} \left[ \cos(\omega(t_2 - t_1)) \right. \\ &\quad \left. - \frac{1}{T_c} \int_{t_0 - T_c}^{t_0} [\cos(\omega(t_1 - t')) \right. \\ &\quad \left. + \cos(\omega(t_2 - t'))] dt' \right] \end{aligned}$$

$$\begin{aligned}
& + \frac{1}{T_c^2} \int_{t_0-T_c}^{t_0} \int_{t_0-T_c}^{t_0} \\
& \left. \cos(\omega(t' - t'')) dt' dt'' \right] \\
& + \sigma^2 \left[ e^{-\kappa|t_2-t_1|} - \frac{1}{T_c} \int_{t_0-T_c}^{t_0} e^{-\kappa|t_1-t'|} \right. \\
& + e^{-\kappa|t_2-t'|} dt' \\
& + \left. \frac{1}{T_c^2} \int_{t_0-T_c}^{t_0} \int_{t_0-T_c}^{t_0} e^{-\kappa|t'-t''|} dt' dt'' \right] \\
= & \frac{\Omega^2}{2} \left[ \cos(\omega(t_2 - t_1)) \right. \\
& + \frac{1}{\omega T_c} (\sin(\omega(t_1 - t_0))) \\
& - \sin(\omega(t_1 - t_0 + T_c)) \\
& + \frac{1}{\omega T_c} (\sin(\omega(t_2 - t_0))) \\
& - \sin(\omega(t_2 - t_0 + T_c)) \\
& + \left. \frac{1}{\omega^2 T_c^2} (2 - 2 \cos(\omega T_c)) \right] \\
& + \sigma^2 \left[ e^{-\kappa|t_2-t_1|} - \frac{1}{T_c} \int_{t_0-T_c}^{t_0} e^{-\kappa|t_1-t'|} \right. \\
& + e^{-\kappa|t_2-t'|} dt' + \frac{1}{T_c^2} \int_{t_0-T_c}^{t_0} \int_{t_0-T_c}^{t_0} \\
& \left. e^{-\kappa|t'-t''|} dt' dt'' \right]. \quad (C.1)
\end{aligned}$$

Applying successively the rules

$$\sin x - \sin(x + a) = -2 \sin \frac{a}{2} \cos \left( x + \frac{a}{2} \right) \text{ and} \quad (C.2)$$

$$\cos x + \cos(x + a) = 2 \cos \frac{a}{2} \cos \left( x + \frac{a}{2} \right) \quad (C.3)$$

to the first part of this formula yields Eq. (25).

## Appendix 4

The drop in the variance over the correction window (Fig. 6a) is caused by the next to last term in Eq. (25) (substituting  $t_1 = t_2 = t$ ):

$$-\frac{2\sigma^2}{T_c} \int_{t_0-T_c}^{t_0} e^{-\kappa|t-t'|} dt'. \quad (D.1)$$

In this appendix it will be proved that a smaller value of  $T_c$  (i.e., shorter correction window) yields a deeper drop. Consider the magnitude of the drop,  $M$ , at the minimum point (halfway point of the correction interval) as a function of  $T_c$  by setting  $t = t_0 - (T_c/2)$  in Eq. (D.1):

$$M(T_c) = \frac{2\sigma^2}{T_c} \int_{t_0-T_c}^{t_0} e^{-\kappa|t_0 - (T_c/2) - t'|} dt'. \quad (D.2)$$

This function is positive and it has to be proven that it is decreasing in  $T_c$  (i.e., having negative slope), which means that a shorter correction interval yields a deeper drop. To prove  $M'(T_c) < 0$ , we first express Eq. (D.2) as

$$M(T_c) = \frac{4\sigma^2}{\kappa T_c} (1 - e^{-\kappa(T_c/2)}) \quad (D.3)$$

and then take the derivative with respect to  $T_c$ :

$$M'(T_c) = \frac{-4\sigma^2}{\kappa T_c^2} + \frac{4\sigma^2}{\kappa T_c^2} e^{-\kappa(T_c/2)} + \frac{2\sigma^2}{T_c} e^{-\kappa(T_c/2)}. \quad (D.4)$$

To prove that the expression in Eq. (D.4) is negative, we multiply this by  $[\kappa T_c^2/(4\sigma^2)]$  and substitute  $s = \kappa T_c/2$ :

$$\frac{\kappa T_c^2}{4\sigma^2} M'(T_c) = -1 + (1 + s)e^{-s}. \quad (D.5)$$

Note that  $s$  only takes strictly positive values. Now the last expression in Eq. (D.5) is always negative because

$$-1 + (1 + s)e^{-s} < 0 \Leftrightarrow 1 + s < e^s, \quad (D.6)$$

which is true for all  $s > 0$ . This completes the proof: a shorter correction interval (i.e., a smaller value of  $T_c$ ) yields a deeper drop in the variance. Therefore the larger the baseline correction window the more stationary the covariance matrix.

## References

- Chung, K.L., 1993. Elementary Probability Theory with Stochastic Processes. Clarendon Press, New York.
- de Munck, J.C., Vijn, P.C.M., Lopes da Silva, F.H., 1992. A random dipole model for spontaneous brain activity. IEEE Trans. Biomed. Eng. 39 (8), 791–804.
- de Munck, J.C., van Dijk, B.W., 1999. The spatial distribution of spontaneous EEG and MEG, in: Uhl, C. (Ed.), Analysis of Neurophysiological Brain Functioning, Springer, Berlin, pp. 202–228.

- de Munck, J.C., Huizenga, H.M., Waldorp, L.J., Heethaar, R.M., 2002. Estimating stationary dipoles from MEG/EEG data contaminated with spatially and temporally correlated background noise. *IEEE Trans. Signal Proc.* 50 (7), 1565–1572.
- Huizenga, H.M., Molenaar, P.C.M., 1995. Equivalent source estimation of scalp potential fields contaminated by heteroscedastic and correlated noise. *Brain Topogr.* 8, 13–33.
- Huizenga, H.M., de Munck, J.C., Waldorp, L.J., Grasman, R.P.P.P., 2002. Spatiotemporal EEG/MEG source analysis based on a parametric noise covariance model. *IEEE Trans. Biomed. Eng.* 49 (6), 533–539.
- Jaśkowski, P., Verleger, R., 1999. Amplitude and latencies of single-trial ERP's estimated by a maximum-likelihood method. *IEEE Trans. Biomed. Eng.* 46, 987–993.
- Lütkenhöner, B., 1998a. Dipole source localization by means of maximum likelihood estimation. I. Theory and simulations. *Electroenceph. Clin. Neurophysiol.* 106, 314–321.
- Lütkenhöner, B., 1998b. Dipole source localization by means of maximum likelihood estimation. II. Experimental evaluation. *Electroenceph. Clin. Neurophysiol.* 106, 322–329.
- Makeig, S., Westerfield, M., Jung, T.P., Enghoff, S., Townsend, J., Courchesne, E., Sejnowski, T.J., 2002. Dynamic brain sources of visual evoked responses. *Science* 295, 690–694.
- Pham, D.T., Möcks, J., Köhler, W., Gasser, T., 1987. Variable latencies of noisy signals: estimation and testing in brain potential data. *Biometrika* 74, 525–533.
- Sekihara, K., Takeuchi, F., Kuriki, S., Koizumi, H., 1994. Reduction of brain noise influence in evoked neuromagnetic source localization using noise spatial correlation. *Phys. Med. Biol.* 39, 937–946.
- Stirzaker, D., 1994. *Elementary Probability*. Cambridge University Press, Cambridge, MA.
- Truccolo, W.A., Ding, M., Knuth, K.H., Nakamura, R., Bressler, L., 2002. Trial-to-trial variability of cortical evoked responses: implications for the analysis of functional connectivity. *Clin. Neurophysiol.* 113, 206–226.
- Waldorp, L.J., Huizenga, H.M., Dolan, C.V., Molenaar, P.C.M., 2002. Estimated generalized least squares electromagnetic source analysis based on a parametric noise covariance model. *IEEE Trans. Biomed. Eng.* 48 (6), 737–741.